The gravitational billion body problem : Het miljard deeltjes probleem

Bédorf, J.

4 A sparse octree gravitational N-body code that runs entirely on the GPU processor

We present the implementation and performance of a new gravitational N-body tree-code that is specifically designed for the graphics processing unit (GPU)[1] . All parts of the tree-code algorithm are executed on the GPU. We present algorithms for parallel construction and traversing of sparse octrees. These algorithms are implemented in CUDA and tested on NVIDIA GPUs, but they are portable to OpenCL and can easily be used on many-core devices from other manufacturers. This portability is achieved by using general parallel-scan and sort methods. The gravitational tree-code outperforms tuned CPU code during the tree-construction and shows a performance improvement of more than a factor 20 overall, resulting in a processing rate of more than 2.8 million particles per second.

Jeroen Bédorf, Evghenii Gaburov and Simon Portegies Zwart
Journal of Computational Physics, Volume 231, Issue 7, p. 2825-2839, March 2012.

[1] The code is publicly available at:
`http://castle.strw.leidenuniv.nl/software.html`

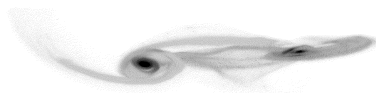

4.1 Introduction

A common way to partition a three-dimensional domain is the use of octrees, which recursively subdivide space into eight octants. This structure is the three-dimensional extension of a binary tree, which recursively divides the one dimensional domain in halves. One can distinguish two types of octrees, namely dense and sparse. In the former, all branches contain an equal number of children and the structure contains no empty branches. A sparse octree is an octree of which most of the nodes are empty (like a sparse matrix), and the structure is based on the underlying particle distribution. In this paper we will only focus on sparse octrees which are quite typical for non-homogenous particle distributions.

Octrees are commonly used in applications that require distance or intersection based criteria. For example, the octree data-structure can be used for the range search method de Berg et al. (2000). On a set of N particles a range search using an octree reduces the complexity of the search from $\mathcal{O}(N)$ to $\mathcal{O}(\log N)$ per particle. The former, though computationally expensive, can easily be implemented in parallel for many particles. The later requires more communication and book keeping when developing a parallel method. Still for large number of particles ($\sim N \geqslant 10^5$) hierarchical[2] methods are more efficient than brute force methods. Currently parallel octree implementations are found in a wide range of problems, among which self gravity simulations, smoothed particle hydrodynamics, molecular dynamics, clump finding, ray tracing and voxel rendering; in addition to the octree data-structure these problems often require long computation times. For high resolution simulations ($\sim N \geqslant 10^5$) 1 (Central Processing Unit) CPU is not sufficient. Therefore one has to use computer clusters or even supercomputers, both of which are expensive and scarce. An attractive alternative is a Graphics Processing Unit (GPU).

Over the years GPUs have grown from game devices into more general purpose compute hardware. With the GPUs becoming less specialised, new programming languages like Brook Buck et al. (2004b), CUDA NVIDIA (2010) and OpenCL Khronos Group Std. (2010) were introduced and allow the GPU to be used efficiently for non-graphics related problems. One has to use these special programming languages in order to be able to get the most performance out of a GPU. This can be realized by considering the enormous difference between today's CPU and GPU. The former has up to 8 cores which can execute two threads each, whereas a modern GPU exhibits hundreds of cores and can execute thousands of threads in parallel. The GPU can contain a large number of cores, because it has fewer resources allocated to control logic compared to a general purpose CPU. This limited control logic renders the GPU unsuitable for non-parallel problems, but makes it more than an order of magnitude faster than the CPU on massively parallel problems NVIDIA (2010). With the recent introduction of fast double precision floating point operations, L1 and L2 caches and ECC memory the GPU has become a major component in the High Performance Computing market. The number of dedicated GPU clusters is steadily increasing and the latest generation of supercomputers have nodes equipped with GPUs, and have established themselves in the upper regions of the top500[3].

This wide spread of GPUs can also be seen in the acceptance of GPUs in computa-

[2] Tree data-structures are commonly referred to as hierarchical data-structures

[3] Top500 Supercomputing November 2010 list, http://www.top500.org

tional astrophysics research. For algorithms with few data dependencies, such as direct N-body simulations, programming the GPU is relatively straightforward. Here various implementations are able to reach almost peak-performance Portegies Zwart et al. (2007); Hamada and Iitaka (2007); Belleman et al. (2008) and with the introduction of N-body libraries the GPU has taken over the GRAPE (GRAvity PipE Makino and Taiji (1998)) [4] as preferred computation device for stellar dynamics Gaburov et al. (2009). Although it is not a trivial task to efficiently utilise the computational power of GPUs, the success with direct N-body methods shows the potential of the GPU in practice. For algorithms with many data dependencies or limited parallelism it is much harder to make efficient use of parallel architectures. A good example of this are the gravitational tree-code algorithms which were introduced in 1986 Barnes and Hut (1986) as a sequential algorithm and later extended to make efficient use of vector machines Barnes (1990). Around this time the GRAPE hardware was introduced which made is possible to execute direct N-body simulations at the same speed as a simulation with a tree-code implementation, while the former scales as $\mathcal{O}(N^2)$ and the latter as $\mathcal{O}(N \log N)$. The hierarchical nature of the tree-code method makes it difficult to parallelise the algorithms, but it is possible to speed-up the computational most intensive part, namely the computation of gravitational interactions. The GRAPE hardware, although unsuitable for constructing and traversing the tree-structure, is able to efficiently compute the gravitational interactions. Therefore a method was developed to create lists of interacting particles on the host and then let the GRAPE solve the gravitational interactions Fukushige et al. (1991); Makino (2004). Recently this method has successfully been applied to GPUs Hamada et al. (2009c,a); Hamada and Nitadori (2010). With the GPU being able to efficiently calculate the force interactions, other parts like the tree-construction and tree-traverse become the bottleneck of the application. Moving the data intensive tree-traverse to the GPU partially lifts this bottleneck Gaburov et al. (2010); Yokota and Barba (2011); (Chapter 3). This method turns out to be effective for shared time-step integration algorithms, but is less effective for block time-step implementations. In a block time-step algorithm not all particles are updated at the same simulation time-step, but only when required. This results in a more accurate (less round-off errors, because the reduced number of interactions) and more efficient (less unnecessary time-steps) simulation. The number of particles being integrated per step can be a fraction of the total number of particles which significantly reduces the amount of parallelism. Also the percentage of time spent on solving gravitational interactions goes down and other parts of the algorithm (e.g. construction, traversal and time integration) become more important. This makes the hierarchical tree N-body codes less attractive, since CPU-GPU communication and tree-construction will become the major bottlenecks Belleman et al. (2008); Gaburov et al. (2010). One solution is to implement the tree-construction on the GPU as has been done for surface reconstruction Zhou et al. (2008) and the creation of bounding volume hierarchies Lauterbach et al. (2009); Pantaleoni and Luebke (2010). An other possibility is is to implement all parts of the algorithm on the GPU using atomic operations and particle insertions Burtscher and Pingali (2011) here the authors, like us, execute all parts of the algorithm on the GPU. When we were in the final stages of finish-

[4] The GRAPE is a plug-in board equipped with a processor that has the gravitational equations programmed in hardware.

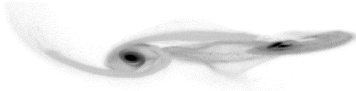

ing the paper we were able to test the implementation by Burtscher et al. Burtscher and Pingali (2011). It is difficult to compare the codes since they have different monopole expansions and multipole acceptance criteria (see Sections 4.3.2 and 4.3.3). However, even though our implementation has higher multipole moments (quadrupole versus monopole) and a more strict multipole acceptance criteria it is at least 4 times faster.

In this work we devised algorithms to execute the tree-construction on the GPU instead of on the CPU as is customarily done. In addition we redesign the tree-traverse algorithms for effective execution on the GPU. The time integration of the particles is also executed on the GPU in order to remove the necessity of transferring data between the host and the GPU completely. This combination of algorithms is excellently suitable for shared and block time-step simulations. Although here implemented as part of a gravitational N-body code (called `Bonsai`, Section 4.3), the algorithms are applicable and extendable to related methods that use hierarchical data structures.

4.2 Sparse octrees on GPUs

The tree construction and the tree-traverse rely on scan algorithms, which can be efficiently implemented on GPUs. (4.A). Here we discuss the main algorithms that can be found in all hierarchical methods. Starting with the construction of the tree-structure in Section 4.2.1, followed by the method to traverse the previously built tree-structure in Section 4.2.2. The methods that are more specific for a gravitational N-body tree-algorithm are presented in Section 4.3.

4.2.1 Tree construction

The common algorithm to construct an octree is based on sequential particle insertion Barnes and Hut (1986) and is in this form not suitable for massively parallel processors. However, a substantial degree of parallelism can be obtained if the tree is constructed layer-by-layer[5] from top to bottom. The construction of a single tree-level can be efficiently vectorised which is required if one uses massively parallel architectures.

To vectorise the tree construction particles have to be mapped from a spatial representation to a linear array while preserving locality. This implies that particles that are nearby in 3D space also have to be nearby in the 1D representation. Space filling curves, which trace through the three dimensional space of the data enable such reordering of particles. The first use of space filling curves in a tree-code was presented by Warren and Salmon (1993) Warren and Salmon (1993) to sort particles in a parallel tree-code for the efficient distribution of particles over multiple systems. This sorting also improves the cache-efficiency of the tree-traverse since most particles that are required during the interactions are stored locally, which improves caching and reduces communication. We adopt the Morton space filling curve (also known as Z-order) Morton (1966), because of the existence of a one-to-one map between N-dimensional coordinates and the corresponding 1D Morton-key. The Morton-keys give a 1D representation of the original ND

[5] A tree-structure is built-up from several layers (also called levels), with the top most level called the root, the bottom levels leaves and in between the nodes.

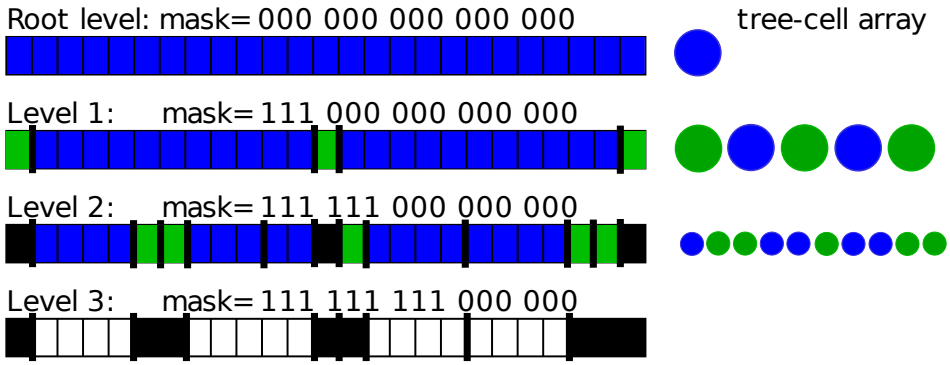

Figure 4.1: Schematic representation of particle grouping into a tree cell. (Left panel) The particles Morton keys are masked[6] with the level mask. Next the particles with the same masked keys are grouped together into cells (indicated by a thick separator, such as in level 1). Cells with less than N_{leaf} particles are marked as leaves (green), and the corresponding particles are flagged (black boxes as in level 2 and 3) and not further used for the tree construction. The other cells are called nodes (blue) and their particles are used constructing the next levels. The tree construction is complete as soon as all particles are assigned to leafs, or when the maximal depth of the tree is reached. (Right panel) The resulting array containing the created tree cells.

coordinate space and are computed using bit-based operations (4.B). After the keys are calculated the particles are sorted in increasing key order to achieve a Z-ordered particle distribution in memory. The sorting is performed using the radix-sort algorithm (see for our implementation details 4.A), which we selected because of its better performance compared to alternative sorting algorithms on the GPU Satish et al. (2009); Merill and Grimshaw (2010). After sorting the particles have to be grouped into tree cells. In Fig. 4.1 (left panel), we schematically demonstrate the procedure. For a given level, we mask the keys[6] of non-flagged particles (non-black elements of the array in the figure), by assigning one particle per GPU thread. The thread fetches the precomputed key, applies a mask (based on the current tree level) and the result is the octree cell to which the particle should be assigned. Particles with identical masked keys are grouped together since they belong to the same cell. The grouping is implemented via the parallel compact algorithm (4.A). We allow multiple particles to be assigned to the same cell in order to reduce the size of the tree-structure. The maximum number of particles that is assigned to a cell is N_{leaf}, which we set to $N_{\text{leaf}} = 16$. Cells containing up-to N_{leaf} particles are marked as leaves, otherwise they are marked as nodes. If a particle is assigned to a leaf the particle is flagged as complete (black elements of the array in the figure). The masking and grouping procedure is repeated for every single level in serial until all particles are assigned to leaves or that the maximal depth of the tree is reached, whichever occurs first. When all particles are assigned to leaves all required tree cells have been created and are stored in a continuous array (right panel of Fig. 4.1).

However, to complete the tree-construction, the parent cells need to be linked to their

[6]The masking is a bitwise operation that preserves the bits which are specified by the mask, for example masking “1011b” with “1100b” results in “1000b”.

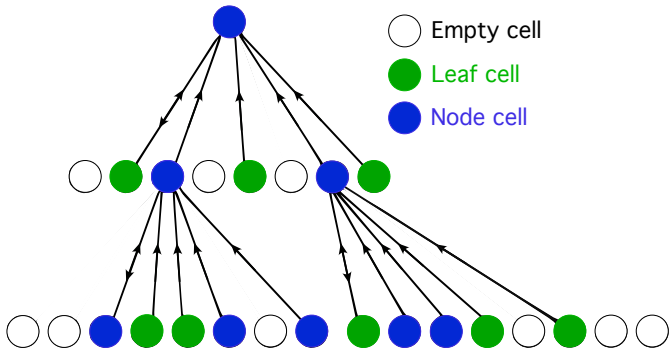

Figure 4.2: Schematic illustration of the tree link process. Each cell of the tree, except the empty cells which are not stored, is assigned to a GPU thread. The thread locates the first child, if it exists, and the parent of the cell. The threads increment the child counter of the parent (indicated by the up arrows) and store the first child in the memory of the cell. This operation requires atomic read-modify-write operations because threads concurrently modify data at the same memory location.

children. We use a separate function to connect the parent and child cells with each other (linking the tree). This function assigns a cell to a single thread which locates its parent and the first child if the cell is not a leaf (Fig. 4.2). This is achieved by a binary search of the appropriate Morton key in the array of tree-cells, which is already sorted in increasing key order during the construction phase. The thread increases the child counter of its parent cell and stores the index of the first child. To reduce memory, we use a single integer to store both the index to the first child and the number of children (most significant 3 bits). If the cell is a leaf, we store the index of the first particle instead of the index of the first child cell, together with the number of particles in the leaf. During these operations many threads concurrently write data to the same memory location. To prevent race conditions, we apply atomic read-modify-write instructions for modifying the data. At the end of this step, the octree is complete and can be used to compute gravitational attractions.

4.2.2 Tree traverse

To take advantage of the massively parallel nature of GPUs we use breadth first, instead of the more common depth first, traversal. Both breadth first and depth first can be parallelised, but only the former can be efficiently vectorised. To further vectorise the calculation we do not traverse a single particle, but rather a group of particles. This approach is known as Barnes' vectorisation of the tree-traverse Barnes (1990). The groups are based on the tree-cells to take advantage of the particle locality as created during the tree-construction. The number of particles in a group is $\leqslant N_{\text{crit}}$ which is typically set to 64 and the total number of groups is N_{groups}. The groups are associated with a GPU thread-block where the number of threads in a block is N_{block} with $N_{\text{block}} >= N_{\text{crit}}$. Hereby we assume that thousands of such blocks are able to run in parallel. This assumption is valid for CUDA-enabled GPUs, as well as on AMD Radeon GPUs via OpenCL. If the code is executed with shared time-steps, all particles are updated at the same time and subsequently all groups are marked as active, for block time-steps this number varies between 1 and N_{groups}.

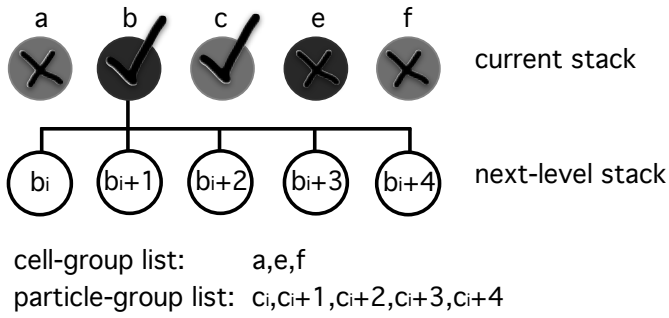

Figure 4.3: Illustration of a single level tree-traverse. There are five cells in the current stack. Those cells which are marked with crosses terminate traverse, and therefore are added to the cell-group list for subsequent evaluation. Otherwise, if the cell is a node, its children are added to the next-level stack. Because children are contiguous in the tree-cell array, they are named as b_i, $b_i + 1$, ..., $b_i + 4$, where b_i is the index of the first child of the node b. If the cell is a leaf, its particles are added to the particle-cell interaction list. Because particles in a leaf are also contiguous in memory, we only need to know the index of the first particle, c_i, and the number of particles in a leaf, which is 5 here.

Each thread block executes the same algorithm but on a different set of particles.

Each thread in a block reads particle data that belongs to the corresponding group as well as group information which is required for the tree traverse. If the number of particles assigned to a group is smaller than N_{block} by a factor of two or more, we use multiple threads (up to 4) per particle to further parallelise the calculations. As soon as the particle and group data is read by the threads we proceed with the tree-traverse.

On the CPU the tree-traverse algorithm is generally implemented using recursion, but on the GPU this is not commonly supported and hard to parallelise. Therefore we use a stack based breadth first tree-traverse which allows parallelisation. Initially, cells from one of the topmost levels of the tree are stored in the current-level stack and the next-level stack is empty; in principle, this can be the root level, but since it consists of one cell, the root node, only one thread from N_{block} will be active. Taking a deeper level prevents this and results in more parallelism. We loop over the cells in the current-level stack with increments of N_{block}. Within the loop, the cells are distributed among the threads with no more than one cell per thread. A thread reads the cell's properties and tests whether or not to traverse the tree further down from this cell; if so, and if the cell is a node the indexes of its children are added to the next-level stack. If however, the cell is a leaf, the indexes of constituent particles are stored in the particle-group interaction list. Should the traverse be terminated then the cell itself is added to cell-group interaction list (Fig.4.3).

The cell-group interaction list is evaluated when the size of the list exceeds N_{block}. To achieve data parallelism each thread reads properties of an interacting cell into fast low-latency on-chip memory that can be shared between the threads, namely shared memory (CUDA) or local memory (OpenCL). Each thread then progresses over the data in the on-chip memory and accumulates partial interactions on its particle. At the end of this pass, the size of the interaction list is decreased by N_{block} and a new pass is started until the size of the list falls below N_{block}. The particle-group interaction list is evaluated in exactly the same way, except that particle data is read into shared memory instead of cell data.

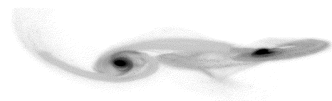

This is a standard data-sharing approach that has been used in a variety of N-body codes, e.g. Nyland et al. Nyland et al. (2007).

The tree-traverse loop is repeated until all the cells from the current-level stack are processed. If the next-level stack is empty, the tree-traverse is complete, however if the next-level stack is non-empty its data is copied to the current-level stack. The next-level stack is cleaned and the current-level stack is processed. When the tree-traverse is complete either the cell-group, particle-group or both interaction lists may be non-empty. In such case the elements in these lists are distributed among the threads and evaluated in parallel. Finally if multiple threads per particle are used an extra reduction step combines the results of these threads to get the final interaction result.

4.3 Gravitational Tree-code

To demonstrate the feasibility and performance, we implement a version of the gravitational Barnes-Hut tree-code Barnes and Hut (1986) which is solely based on the sparse octree methods presented in the previous sections. In contrast to other existing GPU codes Hamada et al. (2009a); Gaburov et al. (2010) and Chapter 3, our implementation runs entirely on GPUs. Apart from the previous described methods to construct and traverse the tree-structure we implement time integration (Section 4.3.1), time-step calculation and tree-cell properties computation on the GPU (Section 4.3.2). The cell opening method, which sets the accuracy and performance of the tree-traverse, is described in Section 4.3.3.

4.3.1 Time Integration

To move particles forward in time we apply the leapfrog predictor-corrector algorithm described by Hut et al. (1995) Hut et al. (1995). Here the position and velocity are predicted to the next simulation time using previously calculated accelerations. Then the new accelerations are computed (tree-traverse) and the velocities are corrected. This is done for all particles in parallel or on a subset of particles in case of the block-time step regime. For a cluster of $\gtrsim 10^5$ particles, the time required for one prediction-correction step is less than 1% of the total execution time and therefore negligible.

4.3.2 Tree-cell properties

Tree-cell properties are a summarized representation of the underlying particle distribution. The multipole moments are used to compute the forces between tree-cells and the particles that traverse the tree. In this implementation of the Barnes-Hut tree-code we use only monopole and quadrupole moments McMillan and Aarseth (1993). Multipole moments are computed from particle positions and need to be recomputed at each time-step; any slowdown in their computation may substantially influence the execution time. To parallelise this process we initially compute the multipole moments of each leaf in parallel. We subsequently traverse the tree from bottom to top. At each level the multipole moments of the nodes are computed in parallel using the moments of the cells one level below (Fig. 4.4). The number of GPU threads used per level is equal to the number of

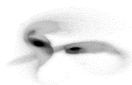

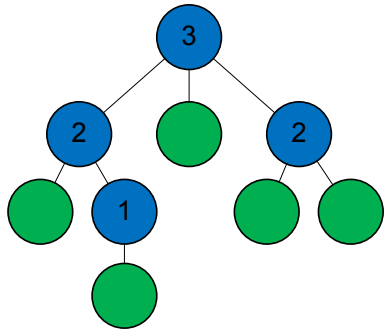

Figure 4.4: Illustration of the computation of the multipole moments. First the properties of the leaves are calculated (green circles). Then the properties of the nodes are calculated level-by-level from bottom to top. This is indicated by the numbers in the nodes, first we compute the properties of the node with number 1, followed by the nodes with number 2 and finally the root node.

nodes at that level. These computations are performed in double precision since our tests indicated that the NVIDIA compiler aggressively optimises single precision arithmetic operations, which results in an error of at most 1% in the multipole moments. Double precision arithmetic solved this problem and since the functions are memory-bound[7] the overhead is less than a factor 2. As final step the double precision values are converted back to single precision to be used during the tree-traverse.

4.3.3 Cell opening criterion

In a gravitational tree-code the multipole acceptance criterion (MAC) decides whether to use the multipole moments of a cell or to further traverse the tree. This influences the precision and execution time of the tree-code. The further the tree is traversed the more accurate the computed acceleration will be. However, traversing the tree further results in a higher execution time since the number of gravitational interactions increases. Therefore the choice of MAC is important, since it tries to determine, giving a set of parameters, when the distance between a particle and a tree cell is large enough that the resulting force approximation error is small enough to be negligible. The MAC used in this work is a combination of the method introduced by Barnes (1994) Barnes (1994) and the method used for tree-traversal on vector machines Barnes (1990). This gives the following acceptance criterion,

$$d > \frac{l}{\theta} + \delta \tag{4.1}$$

where d is the smallest distance between a group and the center of mass of the cell, l is the size of the cell, θ is a dimensionless parameter that controls the accuracy and δ is the distance between the cell's geometrical center and the center of mass. If d is larger than the right side of the equation the distance is large enough to use the multipole moment instead of traversing to the child cells.

Fig. 4.5 gives an overview of this method. We also implemented the minimal distance MAC Salmon and Warren (1994), which results in an acceleration error that is between

[7] On GPUs we distinguish two kind of performance limitations, memory-bound and compute-bound. In the former the performance is limited by the memory speed and memory bandwidth, in the later the performance is limited by the computation speed.

Hardware model	Xeon E5620	8800 GTS512	C1060	GTX285	C2050	GTX480
Architecture	Gulftown	G92	GT200	GT200	GF100	GF100
# Cores	4	128	240	240	448	480
Core (Mhz)	2400	1625	1296	1476	1150	1401
Memory (Mhz)	1066	1000	800	1243	1550	1848
Interface (bit)	192	256	512	512	384	384
Bandwidth (GBs)	25.6	64	102	159	148	177.4
Peak (GFLOPs)[2]	76.8	624	933	1063	1030	1345
Memory size (GB)	16	0.5	4	1	2.5	1.5

[1] All calculations in this work are done in single precision arithmetic.
[2] The peak performance is calculated as follows:
-Gulftown: #Cores × Core speed × 8 (SSE flops/cycle)
-G92 & GT200: #Cores × Core speed × 3 (flops/cycle)
-GF100: #Cores × Core speed × 2 (flops/cycle)

Table 4.1: Used hardware. The Xeon is the CPU in the host system, the other five devices are GPUs.

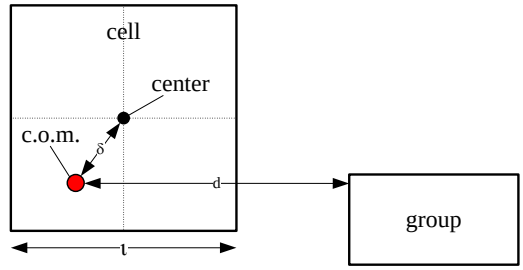

Figure 4.5: Illustration of the computation of the multipole moments. First the properties of the leaves are calculated (green circles). Then the properties of the nodes are calculated level-by-level from bottom to top. This is indicated by the numbers in the nodes, first we compute the properties of the node with number 1, followed by the nodes with number 2 and finally the root node.

10% and 50% smaller for the same θ than the MAC used here. The computation time, however, is almost a factor 3 higher since more cells are accepted (opened).

The accuracy of the tree-traverse is controlled by the parameter θ. Larger values of θ causes fewer cells to be opened and consequently results in a shallower tree-traverse and a faster evaluation of the underlying simulation. Smaller values of θ have the exact opposite effect, but result in a more accurate integration. In the hypothetical case that all the tree cells are opened ($\theta \rightarrow 0$) the tree-code turns in an inefficient direct N-body code. In Section 4.4.1 we adopt $\theta = 0.5$ and $\theta = 0.75$ to show the dependence of the execution time on the opening angle. In Section 4.4.2 we vary θ between 0.2 and 0.8 to show the dependence of the acceleration error on θ.

4.4 Performance and Accuracy

In this section we compare the performance of our implementation of the gravitational N-body code (`Bonsai`) with CPU implementations of comparable algorithms. Furthermore, we use a statistical test to compare the accuracy of `Bonsai` with a direct summation code. As final test `Bonsai` is compared with a direct N-body code and a set of N-body tree-codes using a production type galaxy merger simulation.

Even though there are quite a number of tree-code implementations each has its own specific details and it is therefore difficult to give a one-to-one comparison with other

tree-codes. The implementations closest to this work are the parallel CPU tree-code of John Dubinski (1996) Dubinski (1996) (`Partree`) and the GPU accelerated tree-code `Octgrav` Gaburov et al. (2010), also see Chapter 3. Other often used tree-codes either have a different MAC or lack quadrupole corrections. The default version of `Octgrav` has a different MAC than `Bonsai`, but for the galaxy merger simulation a version of `Octgrav` is used that employs the same method as `Bonsai` (Section 4.3.3). We use `phiGRAPE` Harfst et al. (2007) in combination with the `Sapporo` Gaburov et al. (2009) direct N-body GPU library for the comparison with direct N-body simulations. Although here used as standalone codes, most of them are part of the AMUSE frameworkPortegies Zwart et al. (2009), as will be a future version of `Bonsai` which would make the comparison trivial to execute.

The hardware used to run the tests is presented in Table 4.1. For the CPU calculations we used an Intel Xeon E5620 CPU which has 4 physical cores. For GPUs, we used 1 GPU with the G92 architecture (GeForce 8800GTS512), 2 GPUs with the GT200 architecture (GeForce 285GTX and Tesla C1060), and 2 GPUs with the GF100 architecture (GTX480 and Tesla C2050). All these GPUs are produced by NVIDIA. The Tesla C2050 GPU is marketed as a professional High Performance Computing card and has the option to enable error-correcting code memory (ECC). With ECC enabled extra checks on the data are conducted to prevent the use of corrupted data in computations, but this has a measurable impact on the performance. Therefore, the tests on the C2050 are executed twice, once with and once without ECC enabled to measure the impact of ECC.

All calculations are conducted in single precision arithmetic except for the computation of the monopole and quadrupole moments in `Bonsai` and the force calculation during the acceleration test in `phiGRAPE` for which we use double precision arithmetic.

4.4.1 Performance

To measure the performance of the implemented algorithms we execute simulations using Plummer Plummer (1915) spheres with $N = 2^{15}$ (32k) up to $N = 2^{24}$ (16M) particles (up to $N = 2^{22}$ (4M) for the GTX480, because of memory limitations). For the most time critical parts of the algorithm we measure the wall-clock time. For the tree-construction we distinguish three parts, namely sorting of the keys (sorting), reordering of particle properties based on the sorted keys (moving) and construction and linking of tree-cells (tree-construction). Furthermore, are timings presented for the multipole computation and tree-traverse. The results are presented in Fig. 4.6. The wall-clock time spend in the sorting, moving, tree-construction and multipole computation algorithms scales linearly with N for $N \gtrsim 10^6$. For smaller N, however, the scaling is sub-linear, because the parallel scan algorithms require more than 10^5 particles to saturate the GPU. The inset of Fig. 4.6 shows that the average number of particle-cell interactions doubles between $N \gtrsim$ 32k and $N \lesssim$ 1M and keeps gradually increasing for $N \gtrsim$ 1M. Finally, more than 90% with $\theta = 0.75$ and 95% with $\theta = 0.5$ of the wall-clock time is spent on tree-traversal. This allows for block time-step execution where the tree-traverse time is reduced by a factor $N_{\text{groups}}/N_{\text{active}}$, where N_{active} is the number of groups with particles that have to be updated.

In Fig. 4.7 we compare the performance of the tree-algorithms between the three gen-

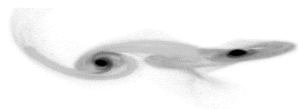

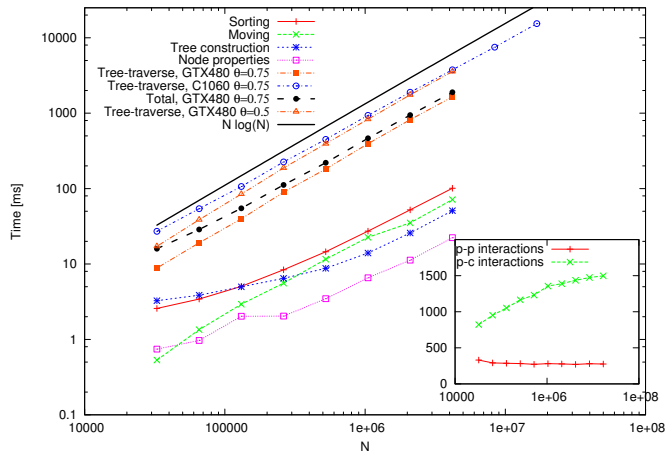

Figure 4.6: The wall-clock time spent by various parts of the program versus the number of particles N. We used Plummer models as initial conditions Plummer (1915) and varied the number of particles over two orders of magnitude. The solid black line, which is offset arbitrarily, shows the theoretical $\mathcal{O}(N \log N)$ scaling Barnes and Hut (1986). The asymptotic complexity of the tree-construction approaches $\mathcal{O}(N)$, because all the constituent primitives share the same complexity. The tree-construction timing comes from the GTX480. To show that the linear scaling continues we added timing data for the C1060, which allows usage of larger data sets. For the GTX480 we included the results of the tree-traverse with $\theta = 0.5$ and the results of the tree-traverse with $\theta = 0.75$. The inset shows the average number of particle-particle and particle-cell interactions for each simulation where $\theta = 0.75$.

erations of GPUs as well as against tuned CPU implementations[8]. For all algorithms the CPU is between a factor of 2 (data reordering) to almost a factor 30 (tree-traverse) slower than the fastest GPU (GTX480). Comparing the results of the different GPUs we see that the GTS512 is slowest in all algorithms except for the data moving phase, in which the C1060 is the slowest. This is surprising since the C1060 has more on-device bandwidth, but the lower memory clock-speed appears to have more influence than the total bandwidth. Overall the GF100 generation of GPUs have the best performance. In particular, during the tree-traverse part, they are almost a factor 2 faster than the GT200 series. This is more than their theoretical peak performance ratios, which are 1.1 and 1.25 for C1060 vs. C2050 and GTX285 vs. GTX480 respectively. In contrast, the GTX285 executes the tree-traverse faster than the C1060 by a factor of 1.1 which is exactly the peak performance ratio between these GPUs. We believe that the difference between the GT200 and GF100 GPUs is mainly caused by the lack of L1 and L2 caches on GT200 GPUs that are present on GF100 GPUs. In the latter, non-coalesced memory accesses are cached, which occur frequently during the tree-traverse, this reduces the need to request data from the

[8] The tree-construction method is similar to Warren and Salmon (1993), and was implemented by Keigo Nitadori with OpenMP and SSE support. The tree-traverse is, however, from the CPU version of the MPI-parallel tree-code by John Dubinski Dubinski (1996). It has monopole and quadrupole moments and uses the same multipole acceptance criterion as our code. We ran this code on the Xeon E5620 CPU using 4 parallel processes where each process uses one of the 4 available physical cores.

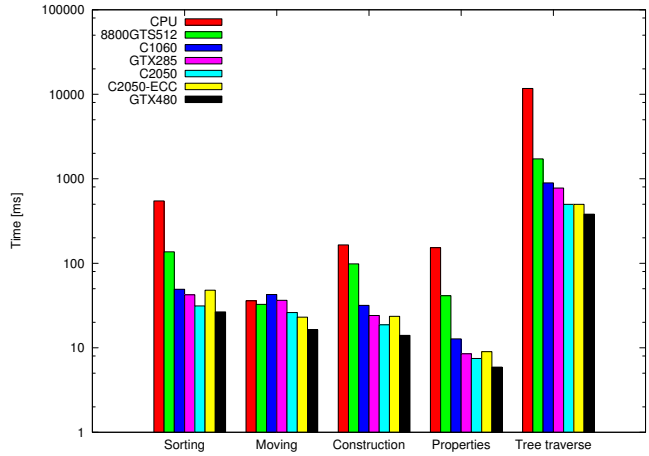

Figure 4.7: Wall-clock time spent by the CPU and different generations of GPUs on various primitive algorithms. The bars show the time spent on the five selected sections of code on the CPU and 5 different GPUs (spread over 3 generations). The results indicate that the code outperforms the CPU on all fronts, and scales in a predictable manner between different GPUs. The `C2050-ECC` bars indicate the runs on the C2050 with ECC enabled, the `C2050` bars indicate the runs with ECC disabled. Note that the y-axis is in log scale. (Timings using a 2^{20} million body Plummer sphere with $\theta = 0.75$)

relatively slow global memory. This is supported by auxiliary tests where the texture cache on the GT200 GPUs is used to cache non-coalesced memory reads, which resulted in a reduction of the tree-traverse execution time between 20 and 30%. Comparing the C2050 results with ECC-memory to those without ECC-memory we notice a performance impact on memory-bound functions that can be as high as 50% (sorting), while the impact on the compute-bound tree-traverse is negligible, because the time to perform the ECC is hidden behind computations. Overall we find that the implementation scales very well over the different GPU generations and makes optimal use of the newly introduced features of the GF100 architecture. The performance of the tree-traverse with $\theta = 0.75$ is 2.1M particles/s and 2.8M particles/s on the C2050 and GTX480 respectively for N = 1M.

4.4.2 Accuracy

To measure the accuracy of the tree-code we use two tests. In the first, the accelerations due to the tree-code are compared with accelerations computed by direct summation. In the second test, we compared the performance and accuracy of three tree-codes and a direct summation code using a galaxy merger simulation.

Acceleration

To quantify the error in the accelerations between `phiGRAPE` and `Bonsai` we calculate

$$\Delta a/a = |\mathbf{a}_{\text{tree}} - \mathbf{a}_{\text{direct}}|/|\mathbf{a}_{\text{direct}}|, \tag{4.2}$$

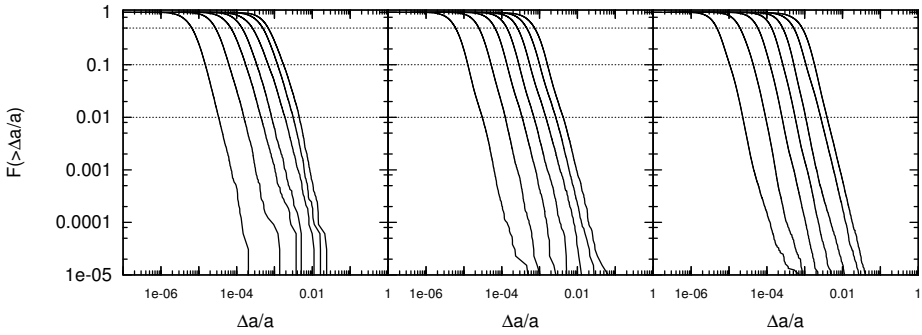

Figure 4.8: Each panel displays a fraction of particles, $F(> \Delta a/a)$, having a relative acceleration error, $\Delta a/a$, (vertical axis) greater than a specified value (horizontal axis). In each panel the solid lines show the errors for various opening angles, from left to right $\theta = 0.2$, 0.3, 0.4, 0.5, 0.6, 0.7 and 0.8. The panels show, from left to right, simulations with $N = 32768$, $N = 131072$ and $N = 1048576$ particles. The dotted horizontal lines indicate 50%, 10% and 1% of the error distribution.

where $\mathbf{a}_{\text{tree}}$ and $\mathbf{a}_{\text{direct}}$ are accelerations obtained by tree and direct summation respectively. The direct summation results are computed with a double precision version of `Sapporo`, while for tree summation single precision is used. For both methods the softening is set to zero and a GTX480 GPU is used as computation device.

In Fig. 4.8 the error distribution for different particle numbers and opening angles is shown. Each panel shows the fraction of particles (vertical-axis) having a relative acceleration error larger than a given value (horizontal-axis). The three horizontal dotted lines show the 50th, 10th and 1st percentile of the cumulative distribution (top to bottom). The results indicate that the acceleration error is slightly smaller (less than an order of magnitude) than `Octgrav` and comparable to CPU tree-codes with quadrupole corrections Dehnen (2002); Springel et al. (2001); Stadel (2001). In `Octgrav` a different MAC is used than in `Bonsai` which explains the better accuracy results of `Bonsai`.

The dependence of the acceleration error on θ and the number of particles is shown in Fig. 4.9. Here the median and first percentile of the relative acceleration error distributions of Fig. 4.8 are plotted as a function of θ. The figure shows that the relative acceleration error is nearly independent of N, which is a major improvement compared to `Octgrav` where the relative acceleration error clearly depends on N (Figure 5 in Gaburov et al. (2010)). The results are consistent with those of `Partree` Dubinski (1996) which uses the same MAC.

Galaxy merger

A realistic comparison between the different N-body codes, instead of statistical tests only, is performed by executing a galaxy merger simulation. The merger consists of two galaxies, each with 10^5 dark matter particles, 2×10^4 star particles and one super massive black hole (for a total of 240.002 bodies). The galaxies have a 1:3 mass ratio and the pericenter is 10kpc. The merger is simulated with `Bonsai, Octgrav, Partree` and `phiGRAPE`. The used hardware for `Bonsai` and `Octgrav` was 1 GTX480, `Partree` used 4 cores of

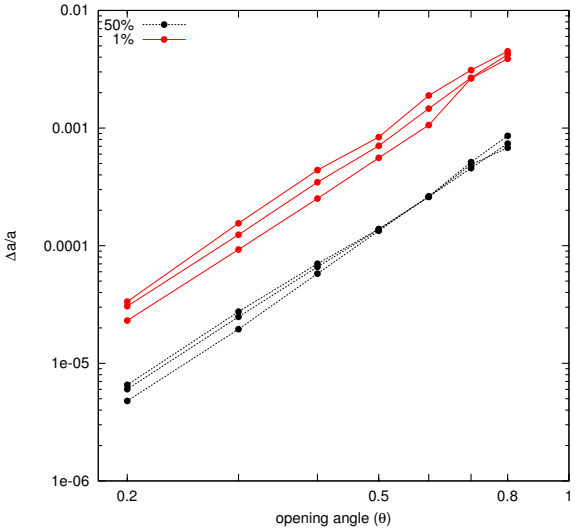

Figure 4.9: The median and the first percentile of the relative acceleration error distribution as a function of the opening angle and the number of particles. We show the lines for $N = 32768$ (bottom striped and solid line) $N = 131072$ (middle striped and dotted line) and $N = 1048576$ (top striped and dotted line).

the Intel Xeon E5620 and `phiGRAPE` used 4 GTX480 GPUs. With each tree-code we ran two simulations, one with $\theta = 0.5$ and one with $\theta = 0.75$. The end-time of the simulations is $T = 1000$ with a shared time-step of $\frac{1}{64}$ (resulting in 64000 steps) and a gravitational softening of $\epsilon = 0.1$. For `phiGRAPE` the default time-step settings were used, with the maximum time-step set to $\frac{1}{16}$ and softening set to $\epsilon = 0.1$. The settings are summarised in the first four columns of Table 4.2.

We compared the density, cumulative mass and circular velocity profiles of the merger product as produced by the different simulation codes, but apart from slight differences caused by small number statistics the profiles are identical. As final comparison we recorded the distance between the two black holes over the course of the simulation. The results of which are shown in the bottom panel of Fig. 4.10, the results are indistinguishable up to the third pericenter passage at $t = 300$ after which the results, because of numerical differences, become incomparable. Apart from the simulation results we also compare the energy conservation. This is done by computing the relative energy error (dE, Eq. 4.3) and the maximal relative energy error (dE_{max}).

$$dE = \frac{E_0 - E_t}{E_0} \tag{4.3}$$

Here E_0 is the total energy (potential energy + kinetic energy) at the start of the simulation and E_t is the total energy at time t. The time is in N-body units.

The maximal relative energy error is presented in the top panel of Fig. 4.10, the tree-code simulations with $\theta = 0.75$ give the highest dE_{max} which occurs for both $\theta = 0.75$ and $\theta = 0.5$ during the second pericenter passage at $t \approx 280$. For $\theta = 0.5$, the dE_{max} is roughly a factor 2 smaller than for $\theta = 0.75$. For `phiGRAPE` dE_{max} shows a drift and does not stay constant after the second pericenter passage. The drift in the energy error is caused by the formation of binaries, for which `phiGRAPE` has no special treatment, resulting in the observed drift instead of a random walk.

Simulation	Hardware	dt	θ	dE_{end} $[\times 10^{-4}]$	dE_{max} $[\times 10^{-4}]$	time [s]
phiGRAPE	4x GTX480	block	-	-1.9	1.8	62068
Bonsai run1	1x GTX480	$\frac{1}{64}$	0.75	0.21	2.8	7102
Bonsai run2	1x GTX480	$\frac{1}{64}$	0.50	0.44	1.3	12687
Octgrav run1	1x GTX480	$\frac{1}{64}$	0.75	-1.1	3.5	11651
Octgrav run2	1x GTX480	$\frac{1}{64}$	0.50	-1.1	2.2	15958
Partree run1	Xeon E5620	$\frac{1}{64}$	0.75	-3.5	3.8	118424
Partree run2	Xeon E5620	$\frac{1}{64}$	0.50	0.87	0.96	303504

Table 4.2: Settings and results of the galaxy merger. The first two columns indicate the software and hardware used, the third the time-step (dt) and the fourth the opening angle (θ). The last three columns present the results, energy error at the $time = 1000$ (fifth column), maximum energy error during the simulation (sixth column) and the total execution time (seventh column).

A detailed overview of the energy error is presented in Fig. 4.11 which shows the relative energy error (dE) over the course of the simulation. Comparing the dE of the tree-codes shows that `Bonsai` has a more stable evolution than `Octgrav` and `Partree`. Furthermore if we compare the results of $\theta = 0.75$ and $\theta = 0.5$ there hardly is any improvement visible for `Octgrav` while `Bonsai` and `Partree` show an energy error with smaller per time-step variance of the energy error.

The last thing to look at is the execution time of the various codes, which can be found in the last column of Tab. 4.2. Comparing `Bonsai` with `Octgrav` shows that the former is faster by a factor of 1.6 and 1.26 for $\theta = 0.75$ and $\theta = 0.5$ respectively. The smaller speed-up for $\theta = 0.5$ results from the fact that the tree-traverse, which takes up most of the execution time, is faster in `Octgrav` than in `Bonsai`. Comparing the execution time of `Bonsai` with that of `Partree` shows that the former is faster by a factor of 17 (24) with $\theta = 0.75$ ($\theta = 0.5$). Note that this speed-up is smaller than reported in Section 4.4.1 due to different initial conditions. Finally, when comparing `phiGRAPE` with `Bonsai`, we find that `Bonsai` completes the simulation on 1 GTX480 faster than `phiGRAPE`, which uses 4 GTX480 GPUs, by a factor of 8.7 ($\theta = 0.75$) and 4.9 ($\theta = 0.5$).

4.5 Discussion and Conclusions

We have presented algorithms to construct and traverse hierarchical data-structures efficiently. These algorithms are implemented as part of a gravitational N-body tree-code. In contrast to other existing GPU tree-codes, this implementation is executed on the GPU. While the code is written in CUDA, the methods themselves are portable to other massively parallel architectures, provided that parallel scan-algorithms exist for such architectures. For this implementation a custom CUDA API wrapper is used that can be replaced with an OpenCL version. As such the code can be ported to OpenCL, by only rewriting the GPU functions, which is currently work in progress.

The number of particles processed per unit time, is 2.8 million particles per second with $\theta = 0.75$ on a GTX480. Combined with the stable energy evolution and efficient

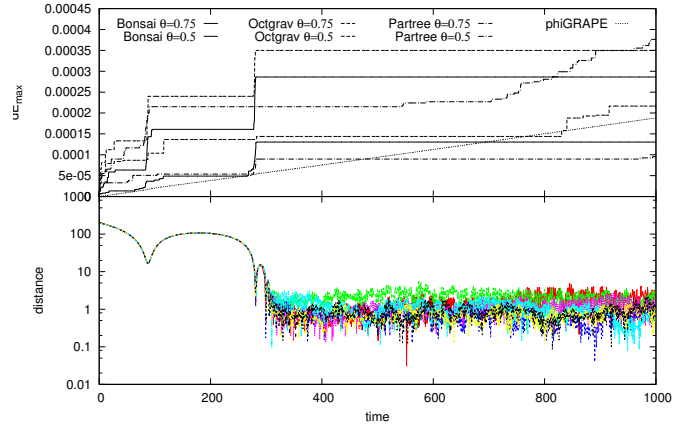

Figure 4.10: The top panel shows the maximal relative energy error over the course of the simulation. The solid lines show the results of `Bonsai`, the striped lines the results of `Octgrav` and the striped-dotted lines show the results of `Partree`. In all cases the top lines show the result of $\theta = 0.75$ and the bottom lines the result of $\theta = 0.5$. Finally the dotted line shows the result of `phiGRAPE`. The bottom panel shows the distance between the two supermassive black-holes. The lines themselves have no labels since up to $t = 300$ the lines follow the same path and after $t = 300$ the motion becomes chaotic and incomparable. The distance and time are in N-body units.

scaling permits us to routinely carry out simulations on the GPU. Since the current version can only use 1 GPU, the limitation is the amount of memory. For 5 million particles ± 1 gigabyte of GPU memory is required.

Although the the tree-traverse in `Octgrav` is $\pm 10\%$ faster than in `Bonsai`, the latter is much more appropriate for large ($N > 10^6$) simulations and simulations which employ block-time steps. In `Octgrav` the complete tree-structure, particle array and multipole moments are send to the GPU during each time-step. When using shared-time steps this is a non-critical amount of overhead since the overall performance is dominated by the tree-traverse which takes up more than 90% of the total compute time. However, this balance changes if one uses block time-steps. The tree-traverse time is reduced by a factor $N_{\rm groups}/N_{\rm active}$, where $N_{\rm active}$ is the number of groups with particles that have to be updated. This number can be as small as a few percent of $N_{\rm groups}$, and therefore tree-construction, particle prediction and communication becomes the bottleneck. By shifting these computations to the GPU, this ceases to be a problem, and the required host communication is removed entirely.

Even though the sorting, moving and tree-construction parts of the code take up roughly 10% of the execution time, these methods do not have to be executed during each time-step when using the block time-step method. It is sufficient to only recompute the multipole moments of tree-cells that have updated child particles. Only when the tree-traverse shows a considerable decline in performance the complete tree-structure has to be rebuild. This decline is the result of inefficient memory reads and an increase of the average number of particle-cell and particle-particle interactions. This quantity in-

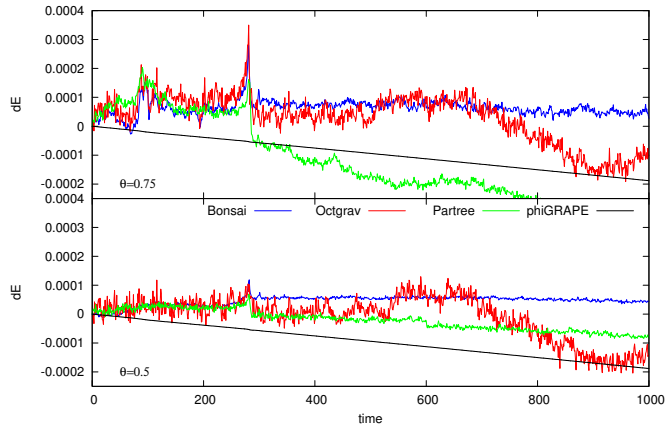

Figure 4.11: Relative energy error over the course of the simulation. The top panel shows the results of $\theta = 0.75$ and the bottom panel the results of $\theta = 0.5$, all other settings as defined in Tab. 4.2. The `Bonsai` results are shown by the blue lines, the `Octgrav` results are shown by the red lines, the `Partree` results are shown by the green lines and the black lines show the results of `phiGRAPE`. Note that the result of `phiGRAPE` is the same in the top and bottom panel and that the range of the y-axis is the same in both panels.

creases because the tree-cell size (l) increases, which causes more cells to be opened by the multipole acceptance criterion (Eq. 4.1).

Although the algorithms described herein are designed for a shared-memory architecture, they can be used to construct and traverse tree-structures on parallel GPU clusters using the methods described in Warren and Salmon (1993); Dubinski (1996). Furthermore, in case of a parallel GPU tree-code, the CPU can exchange particles with the other nodes, while the GPU is traversing the tree-structure of the local data. In this way, it is possible to hide most of the communication time.

The presented tree-construction and tree-traverse algorithms are not limited to the evaluation of gravitational forces, but can be applied to a variety of problems, such as neighbour search, clump finding algorithms, fast multipole method and ray tracing. In particular, it is straightforward to implement Smoothed Particle Hydrodynamics in such a code, therefore having a self-gravitating particle based hydrodynamics code implemented on the GPU.

Acknowledgements

This work is supported by NOVA and NWO grants (#639.073.803, #643.000.802, #614.061.608, #643.200.503, VIDI #639.042.607). The authors would like to thank Massimiliano Fatica and Mark Harris of NVIDIA for the help with getting the code to run on the Fermi architecture, Bernadetta Devecchi for her help with the galaxy merger simulation and Dan Caputo for his comments which improved the manuscript.

4.A Scan algorithms

Both tree-construction and tree-traverse make extensive use of parallel-scan algorithms, also known as parallel prefix-sum algorithms. These algorithms are examples of computations that seem inherently sequential, but for which an efficient parallel algorithm can be defined. Blelloch Guy E. Blelloch (1990) defines the scan operations as follows:

Definition: *The* all-prefix-sums *operation takes a binary associative operator* $\oplus$*, and an array of n elements*

$$[a_0, a_1, ..., a_{n-1}],$$

and returns the ordered set

$$[a_0,(a_0 \oplus a_1), ...,(a_0 \oplus a_1 \oplus ... \oplus a_{n-1})].$$

Example: If $\oplus$ is the addition operator, then the all-prefix-sums operation on the array

$$[3\ 1\ 7\ 0\ 4\ 1\ 6\ 3],$$

would return

$$[3\ 4\ 11\ 11\ 15\ 16\ 22\ 25].$$

The prefix-sum algorithms form the building blocks for a variety of methods, including stream compaction, stream splitting, sorting, regular expressions, tree-depth determination and histogram construction. In the following paragraphs, we give a concise account on the algorithms we used in this work, however we refer the interested readers to the survey by Blelloch Guy E. Blelloch (1990) for further examples and detailed descriptions.

4.A.1 Stream Compaction

Stream compaction removes "invalid" items from a stream of elements; this algorithm is also known as stream reduction. In the left panel of the Fig.4.12 an example of a compaction is shown where invalid elements are removed and valid elements are placed at the start of the output stream.

4.A.2 Split and Sort

Stream split is related to stream compaction, but differs in that the invalid elements are placed behind the valid ones in the output stream instead of being discarded (right panel of Fig.4.12). This algorithm is used as building block for the radix sort primitive. Namely, for each bit of an integer we call the split algorithm, starting from the least significant bit, and terminating with the most significant bit Knuth (1997).

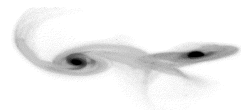

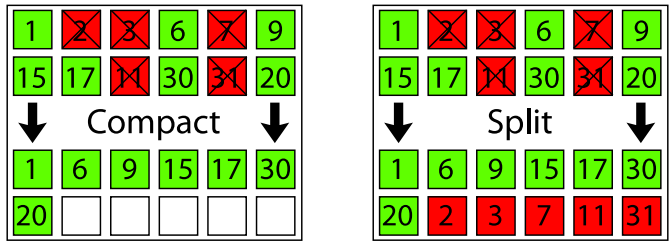

Figure 4.12: Example of compact and split algorithms. The "compact" discards invalid items whereas the "split" places these behind the valid items. We use this "split" primitive for our radix sort implementation because it preserves the item ordering–a property which is fundamental for the radix sort algorithm.

4.A.3 Implementation

All parts of our parallel octree algorithms use scan algorithms in one way or another. Therefore, it is important that these scan algorithms are implemented in the most efficient way and do not become the bottleneck of the application. There are many different implementations of scan algorithms on many-core architectures Mark Harris (NVIDIA) (2009); Sengupta et al. (2008); Billeter et al. (2009). We use the method of Billeter et al. Billeter et al. (2009) for stream compaction, split and radix-sort because it appears to be, at the moment of writing, the fastest and is easily adaptable for our purposes.

Briefly, the method consists of three steps:

1. Count the number of valid elements in the array.
2. Compute output offsets using parallel prefix-sum.
3. Place valid elements at the output offsets calculated in the previous step.

We used the prefix-sum method described by Sengupta et al. Sengupta et al. (2008), for all such operations in both the tree-construction and tree-traverse parts of the implementation.

4.B Morton Key generation

One of the properties of the Morton key is its direct mapping between coordinates and keys. To generate the keys given a set of coordinates one can make use of look-up tables or generate the keys directly. Since the use of look-up tables is relative inefficient on GPUs (because of the many parallel threads that want to access the same memory) we decided to compute the keys directly. First we convert the floating point positions into integer positions. This is done by shifting the reference frame to the lower left corner of the domain and then multiply the new positions by the size of the domain. Then we can apply bit-based dilate primitives to compute the Morton key (List.4.1, Raman and Wise (2008)). This dilate primitive converts the first 10 bits of an integer to a 30 bit representation, i.e. `0100111011` → `000 001 000 000 001 001 001 000 001 001`:

List 4.1: The GPU code which we use to dilate the first 10-bits of an integer.

```
int dilate(const int value) {
  unsigned int x;
  x = value & 0x03FF;
  x = ((x << 16) + x) & 0xFF0000FF;
  x = ((x <<  8) + x) & 0x0F00F00F;
  x = ((x <<  4) + x) & 0xC30C30C3;
  x = ((x <<  2) + x) & 0x49249249;
  return x;
}
```

This dilate primitive is combined with bit-shift and `OR` operators to get the particles' key. In our implementation, we used 60-bit keys, which is sufficient for an octree with the maximal depth of 20 levels. We store a 60-bit key in two 32-bit integers, each containing 30-bits of the key. The maximal depth imposes a limit on the method, but so far we have never run into problems with our simulations. This limitation can easily be lifted by either going to 90-bit keys for 30 levels or by modifying the tree-construction algorithm when we reach deepest levels. This is something we are currently investigating.